Nuclear Engineering and Technology 51 (2019) 1444–1450

Contents lists available at ScienceDirect

Nuclear Engineering and Technology

journal homepage: www.elsevier.com/locate/net

Original Article

Neutron-shielding behaviour investigations of some clay-materials

S.F. Olukotun [a, *], Kulwinder Singh Mann [b], S.T. Gbenu [c], F.I. Ibitoye [c], O.F. Oladejo [d], Amit Joshi [e], H.O. Tekin [f], M.I. Sayyed [g], M.K. Fasasi [c], F.A. Balogun [c], Turgay Korkut [h]

[a] Department of Physics and Engineering Physics, Obafemi Awolowo University, Ile-Ife, Nigeria
[b] Department of Physics, D.A.V College, Bathinda, 151001, Punjab, India
[c] Centre for Energy Research and Development (CERD), Obafemi Awolowo University, Ile-Ife, Nigeria
[d] Department of Mathematical and Physical Science, Osun State University, Osogbo, Nigeria
[e] Department of Physics, Guru-Kashi University, Talwandi-Sabo, Punjab, India
[f] Radiotherapy Department, Üsküdar University, Vocational School of Health Services, Istanbul, 34672, Turkey
[g] Physics Department, Faculty of Science, University of Tabuk, Saudi Arabia
[h] Department of Nuclear Energy Engineering, Faculty of Engineering, Sinop University, 57000, Sinop, Turkey

ARTICLE INFO

Article history:
Received 23 December 2017
Received in revised form
15 February 2019
Accepted 31 March 2019
Available online 24 April 2019

Keywords:
Composite materials
Effective removal cross-section
Mass removal cross section
Mean free path
Fast-neutrons
WinNC-toolkit
PIXE
MCNPX
GEANT4

ABSTRACT

The fast-neutron shielding behaviour (FNSB) of two clay-materials (Ball clay and Kaolin)of Southwestern Nigeria (7.49°N, 4.55°E) have been investigated using effective removal cross section, $\Sigma_R(cm^{-1})$, mass removal cross section, $\Sigma_{R/\rho}(cm^2g^{-1})$ and Mean free path, λ (cm). These parameters decide neutron shielding behaviour of any material. A computer program - WinNC-Toolkit has been used for computation of these parameters. The toolkit evaluates these parameters by using elemental compositions and densities of samples. The proficiency of WinNC-Toolkit code was probe by using MCNPX and GEANT4 to model fast neutron transmission of the samples under narrow beam geometry, intending to represent the actual experimental setup. Direct calculation of effective removal cross section (cm^{-1}) of the samples was also carried out. The results from each of the methods for each types of the studied clay-materials (Ball clay and Kaolin) shows similar trend. The trend might be the fingerprint of water content retained in each of the samples being baked at different temperature. The compositions of each sample have been obtained by Particle-Induced X-ray Emission (PIXE) technique (Tandem Pelletron Accelerator: 1.7 MV, Model 5SDH). The FNSB of the selected clay-materials have been compared with standard concrete. The cognizance of various factors such as availability, thermo-chemical stability and water retaining ability by the clay-samples can be analyzed for efficacy of the material for their FNSB.

1. Introduction

The nuclear-technology is useful in several fields such as industry, medicine, agriculture and scientific research. It is a reliable and clean power-source [1]. Besides numerous advantages of this technology some precautions should be taken to avoid the exposure to hazardous ionizing-radiations such as neutrons, gamma-rays, charged-particles and fission-fragments. The risk of radiation-hazard put major restriction on excessive use nuclear-technology to fulfill the increasing demand of power.

Various studies have shown that exposure to the ionizing-radiations can cause havoc to both living and non-living things [2–4]. This potential radiation risk must be assessed and controlled to minimize the menace to the public and associated property [3]. During reactor-shielding, the shielding of neutrons and γ-rays are the major concern. Since any material that attenuates neutrons and γ-rays, effectively attenuates other type of nuclear-radiations [4–10].

According to Oak ridge national laboratory [11], origin of radiation shielding research can be intimately tied to the operation of the world's first self-sustaining chain nuclear reactor during the year 1943. Several materials have been investigated for the radiation-shielding purpose. Beside from good radiation-shielding behaviour of a material, it should possess necessary physiochemical properties such as melting point, corrosion, thermo-chemical instability etc. Thus, for innovatory applications of the nuclear-technology in different fields necessitate the continuous search for better shielding-materials.

* Corresponding author.
E-mail addresses: olukotunsf@oauife.edu.ng, olukotunsf@yahoo.com (S.F. Olukotun).

https://doi.org/10.1016/j.net.2019.03.019

It has been discovered that Clays have all the desired physiochemical properties for good shielding-materials such as high melting point, good thermo-chemical stability, and higher mechanical strength at an elevated temperature, better shock resistance and high resistance to corrosion [12,13]. Interestingly, Clay constituents low-Z elements and has good capability to retain water (H_2O). These properties make it suitable for neutron-shielding [6]. On the other hand, Clay-materials are abundantly available thus proves to be cost-effective and eco-friendly composite-material [14].

In this study fast-neutron-shielding behaviour (FNSB) for clay-materials found at Ile-Ife (South-western Nigeria has been carried out. Various shielding parameters such as effective fast-neutrons removal cross section, $\Sigma_R(cm^{-1})$, mass removal cross section, $\Sigma_{R/\rho}(cm^2g^{-1})$ and mean free path, λ (cm) have been used to ascertain FNSB. These parameters have been computed using WinNC-Toolkit; MCNPX; GEANT4 and direct calculation [15–17]. For neutron energies between 2 and 12 MeV, the effective removal cross-section is considered to be approximately constant [18]. Various researchers [7–10,19–21] have confirmed that these parameters provide good information regarding neutron-shielding behaviour of sample-material.

2. Theoretical method

WinNC-toolkit has been designed to provide theoretical

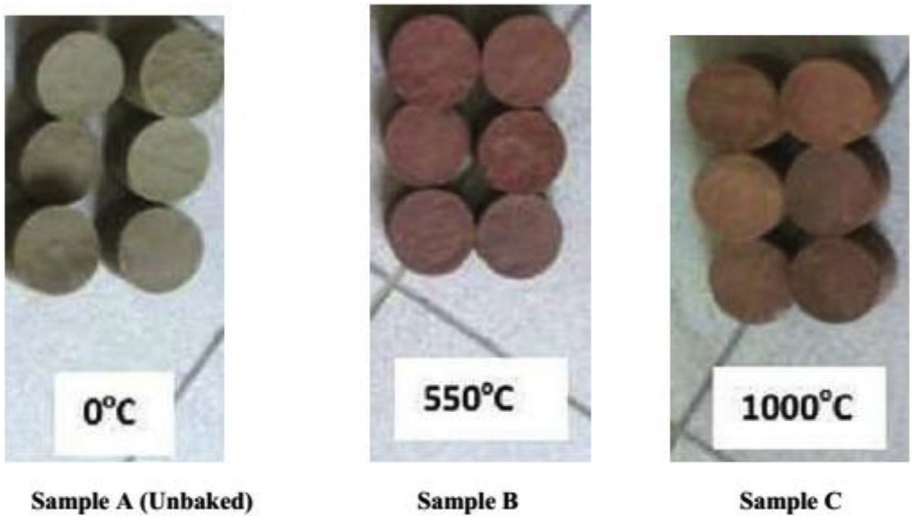

Fig. 1. Ball clay baked at different temperature.

Fig. 2. Kaolin baked at different temperature.

Table 1
Comparison of WinNC-Toolkit results with literature values for the validation of the code.

Concrete Samples	Density (gcm^{-3})	Measured values of Σ_R (cm^{-1})		
		WinNC-Toolkit [15]	Manual Calculation [15, 43]	Experimental Measurement[15, 43]
Ordinary-concrete	2.30	0.0930	0.0937	0.1083
Hematite-serpentine	2.50	0.0978	0.0967	0.1160
Ilmenite-limonite	2.90	0.0943	0.0950	0.1433
Basalt-magnetite	3.05	0.1108	0.1102	0.1270
Ilmenite	3.50	0.1111	0.1121	0.1625
Steel Scrap	4.00	0.1226	0.1247	0.1654
Steel-magnetite	5.11	0.1421	0.1420	0.1680

Table 2
WinNC Output: The $\Sigma_{R/\rho}$, Σ_R and λ of Ball Clay and Kaolin using its Elemental Compositions.

Element	Sample A			Sample B			Sample C			Sample D			Sample E			Sample F		
	Density (gcm^{-3}) = 1.99 λ (cm) = 17.38			Density (gcm^{-3}) = 1.97 λ (cm) = 17.63			Density (gcm^{-3}) = 1.96 λ (cm) = 17.88			Density (gcm^{-3}) = 1.99 λ (cm) = 17.39			Density (gcm^{-3}) = 1.97 λ (cm) = 17.55			Density (gcm^{-3}) = 1.96 λ (cm) = 17.59		
	Ele.Conc By Wt	$\Sigma_{R/\rho}$ (cm^2g^{-1})	Σ_R (cm^{-1})	Ele.Conc By Wt	$\Sigma_{R/\rho}$ (cm^2g^{-1})	Σ_R (cm^{-1})	Ele.Conc By Wt	$\Sigma_{R/\rho}$ (cm^2g^{-1})	Σ_R (cm^{-1})	Ele.Conc By Wt	$\Sigma_{R/\rho}$ (cm^2g^{-1})	Σ_R (cm^{-1})	Ele.Conc By Wt	$\Sigma_{R/\rho}$ (cm^2g^{-1}	Σ_R (cm^{-1})	Ele.Conc By Wt	$\Sigma_{R/\rho}$ (cm^2g^{-1})	Σ_R (cm^{-1})
Mg	1.44E-02	3.33E-02	9.50E-04	1.44E-02	3.33E-02	9.44E-04	1.11E-02	3.33E-02	7.25E-04	0.00E+00	0.00E+00	0.00E+00	0.00E+00	0.00E+00	0.00E+00	0.00E+00	0.00E+00	0.00E+00
Al	3.54E-01	2.93E-02	2.06E-02	2.38E-01	2.93E-02	1.37E-02	2.08E-01	2.93E-02	1.19E-02	3.59E-01	2.93E-02	2.09E-02	3.51E-01	2.93E-02	2.02E-02	3.61E-01	2.93E-02	2.07E-02
Si	5.59E-01	2.95E-02	3.28E-02	6.59E-01	2.95E+02	3.82E-02	6.39E-01	2.95E-02	3.69E-02	5.52E-01	2.95E-02	3.24E-02	5.68E-01	2.95E-02	3.29E-02	5.58E-01	2.95E-02	3.23E-02
P	0.00E+00	0.00E-02	0.00E+00	3.32E-04	2.83E-02	1.84E-05	2.96E-02	2.83E-02	1.64E-03	0.00E+00	0.00E+00	0.00E+00	0.00E+00	0.00E+00	0.00E+00	0.00E+00	0.00E+00	0.00E+00
Cl	6.40E-04	2.52E-02	3.21E-05	4.12E-04	2.52E-02	2.04E-05	4.69E-03	2.52E-02	2.32E-04	7.04E-04	2.52E-02	3.53E-05	0.00E+00	0.00E+00	0.00E+00	0.00E+00	0.00E+00	0.00E+00
K	1.74E-02	2.47E-02	8.56E-04	2.19E-02	2.47E-02	1.06E-03	1.34E-02	2.47E-02	6.46E-04	6.68E-02	2.47E-02	3.28E-03	6.59E-02	2.47E-02	3.20E-03	6.53E-02	2.47E-02	3.16E-03
Ca	2.70E-03	2.43E-02	1.30E-04	3.19E-03	2.43E-02	1.53E-04	2.96E-04	2.43E-02	1.41E-05	2.79E-03	2.43E-02	1.35E-04	1.28E-03	2.43E-02	6.10E-05	1.31E-03	2.43E-02	6.23E-05
Ti	8.58E-03	2.05E-02	3.50E-04	1.09E-02	2.05E-02	4.40E-04	1.97E-04	2.05E-02	7.91E-06	5.12E-04	2.05E-02	2.08E-05	4.73E-04	2.05E-02	1.91E-05	5.04E-04	2.05E-02	2.03E-05
V	1.56E-04	2.13E-02	6.59E-06	0.00E+00	0.00E+00	0.00E-00	8.79E-04	2.13E-02	3.67E-05	0.00E+00	0.00E+00	0.00E+00	0.00E+00	0.00E+00	0.00E+00	7.28E-05	2.13E-02	3.04E-06
Cr	9.88E-05	2.08E-02	4.08E-06	1.21E-04	2.08E-02	4.93E-06	9.23E-02	2.08E-02	3.76E-03	4.76E-05	2.08E-02	1.97E-06	0.00E+00	0.00E+00	0.00E+00	0.00E+00	0.00E+00	0.00E+00
Mn	4.58E-04	2.03E-02	1.85E-05	5.74E-04	2.03E-02	2.29E-05	2.77E-05	2.03E-02	1.10E-06	1.68E-04	2.03E-02	6.76E-06	1.03E-04	2.03E-02	4.11E-06	1.55E-04	2.03E-02	6.17E-06
Fe	4.18E-02	2.14E-02	1.78E-03	4.98E-02	2.14E-02	2.10E-03	1.36E-04	2.14E-02	5.71E-06	1.68E-02	2.14E-02	7.15E-04	1.28E-02	2.14E-02	5.37E-04	1.32E-02	2.14E-02	5.53E-04
Cu	1.51E-05	1.86E-02	5.57E-07	2.53E-05	1.86E-02	9.23E-07	0.00E+00	0.00E+00	0.00E+00	0.00E+00	0.00E+00	0.00E+00	0.00E+00	0.00E+00	0.00E+00	0.00E+00	0.00E+00	0.00E+00
Zn	5.73E-05	1.83E-02	2.09E-06	7.78E-05	1.83E-02	2.80E-06	0.00E+00	0.00E+00	0.00E+00	1.26E-04	1.83E-02	4.60E-06	7.34E-05	1.83E-02	2.64E-06	9.98E-05	1.83E-02	3.58E-06
Rb	1.05E-04	1.63E-02	3.39E-06	1.01E-04	1.63E-02	3.23E-06	1.11E-03	1.63E-02	3.54E-05	6.32E-04	1.63E-02	2.05E-05	4.69E-04	1.63E-02	1.05E-05	5.86E-04	1.63E-02	1.87E-05
Zr	4.56E-04	1.56E-02	1.41E-05	8.61E-04	1.56E-02	2.64E-05	0.00E+00	0.00E+00	0.00E+00	0.00E+00	0.00E+00	0.00E+00	0.00E+00	0.00E+00	0.00E+00	0.00E+00	0.00E+00	0.00E+00
Total	**1.0000**	**0.0290**	**0.0575**	**1.0000**	**0.0289**	**0.0575**	**1.0000**	**0.0286**	**0.0559**	**1.0000**	**0.0289**	**0.0575**	**1.0000**	**0.0290**	**0.0570**	**1.0000**	**0.0290**	**0.568**

information of FNSB using various shielding parameters of the sample (composite materials). This toolkit has been fabricated specifically for fast-neutrons in analogy to WinXCom [22]. It is designed with updated database file of $\Sigma_{R/\rho}(cm^2g^{-1})$ and with some extended capabilities, over the similar existing computer programs (ParShield, MERCSF-N and NXcom). The missing values of $\Sigma_{R/\rho}(cm^2g^{-1})$ for nine elements (Tc, Pm, Po, At, Rn, Fr, Ra, Ac and Pa) in the existing programs have been estimated using bi-quadratic polynomial fitting interpolation method with the Linest function of Microsoft-Excel® [15]. The removal cross section, $\Sigma_R(cm^{-1})$ provides the information of probability that a fast or fission-energy neutron undergoes first collision, which removes it from the group of penetrating uncollided neutrons. While the mean free path λ (cm) is the inverse of $\Sigma_R(cm^{-1})$ it describes the average distance travelled by a neutron between two successive interactions. The mass removal cross section $\Sigma_{R/\rho}(cm^2g^{-1})$ provides neutron-shielding behaviour of sample. For compound or mixture, $\Sigma_{R/\rho}(cm^2g^{-1})$ value is the sum of separate contributions of each of the elements that constitute the compound or mixture. All these parameters for each sample have been evaluated with mixture rule [18,24].

$$\Sigma_{R/\rho} = \sum_i \omega_i \left(\Sigma_{R/\rho}\right)_i \tag{1}$$

$$\Sigma_R = \sum_i \rho_i \left(\Sigma_{R/\rho}\right)_i \tag{2}$$

$$\lambda = \left[\sum_i \rho_i \left(\Sigma_{R/\rho}\right)_i\right]^{-1} \tag{3}$$

$$\rho_i = \omega_i \rho \tag{4}$$

Where ω_i and ρ_i are weight fraction and partial density respectively of the element i.

MCNPX is the Monte Carlo N-Particle eXtended, a version of MCNP code. MCNP is a general-purpose MonteCarlo N-Particle code that can be used for neutron, photon, electron, or coupled

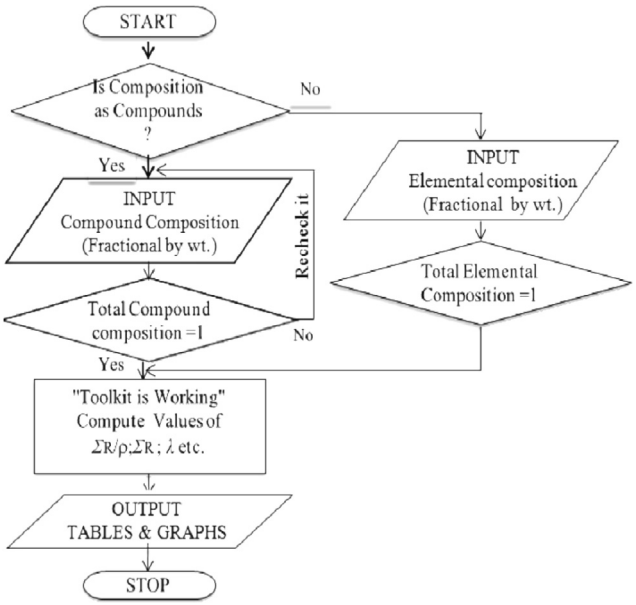

Fig. 3. Flow Chart of WinNC – Toolkit (Mann et al., 2015).

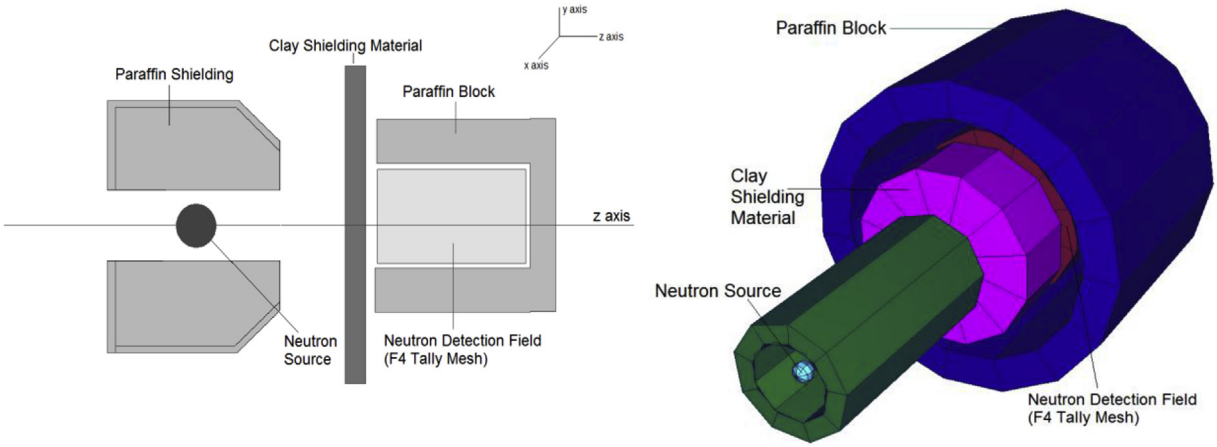

Fig. 4. **(a) S**imulation setup **(b)** 3-D view of set up obtained from MCNPX Visual Editor (Version X_22S).

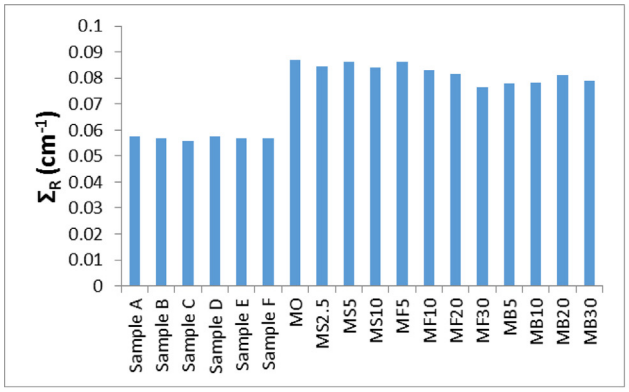

	Name	Samples Description
The Clay-materials	Sample A	Ball Clay baked at 0ºC
	Sample B	Ball Clay baked at 550ºC
	Sample C	Ball Clay baked at 1000ºC
	Sample D	Kaolin baked at 0ºC
	Sample E	Kaolin baked at 550ºC
	Sample F	Kaolin baked at 1000ºC
Concrete materials (Yilmaz, 2011)	MO	Ordinary Concrete
	MS2.5	Concrete made of 2.5% of Silica Fume
	MS5	Concrete made of 5% of Silica Fume
	MS10	Concrete made of 10% of Silica Fume
	MF5	Concrete made of 5% fly ash
	MF10	Concrete made of 10% fly ash
	MF20	Concrete made of 20% fly ash
	MF30	Concrete made of 30% fly ash
	MB5	Concrete made of 5% furnance slag mortal
	MB10	Concrete made of 10% furnance slag mortal
	MB20	Concrete made of 20% furnance slag mortal
	MB30	Concrete made of 30% furnance slag mortal

Fig. 5. The effective removal cross section of the clay-materials and concrete materials.

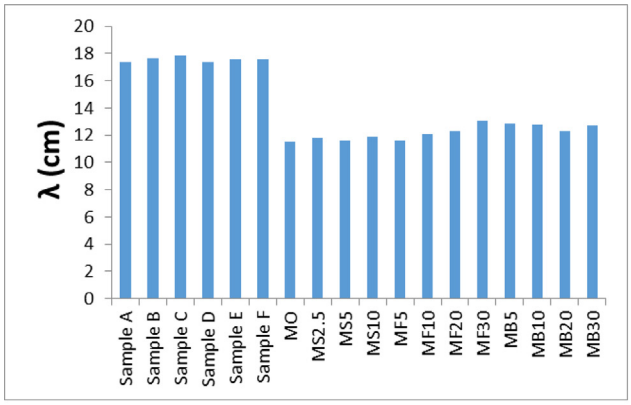

	Name	Samples Description
The Clay-materials	Sample A	Ball Clay baked at 0ºC
	Sample B	Ball Clay baked at 550ºC
	Sample C	Ball Clay baked at 1000ºC
	Sample D	Kaolin baked at 0ºC
	Sample E	Kaolin baked at 550ºC
	Sample F	Kaolin baked at 1000ºC
Concrete materials (Yilmaz, 2011)	MO	Ordinary Concrete
	MS2.5	Concrete made of 2.5% of Silica Fume
	MS5	Concrete made of 5% of Silica Fume
	MS10	Concrete made of 10% of Silica Fume
	MF5	Concrete made of 5% fly ash
	MF10	Concrete made of 10% fly ash
	MF20	Concrete made of 20% fly ash
	MF30	Concrete made of 30% fly ash
	MB5	Concrete made of 5% furnance slag mortal
	MB10	Concrete made of 10% furnance slag mortal
	MB20	Concrete made of 20% furnance slag mortal
	MB30	Concrete made of 30% furnance slag mortal

Fig. 6. The mean free path of the clay-materials and concrete materials.

neutron/photon/electron transport simulation [16]. Specific areas of application include, but are not limited to, radiation protection and dosimetry, radiation shielding, radiography, medical physics, nuclear criticality safety, detector design and analysis, nuclear oil well logging, accelerator target design, fission and fusion reactor design, decontamination and decommissioning [16]. MCNP is distributed by the Radiation Safety Information Computational Center website (RSICC), based at the Oak Ridge National Laboratory in Oak Ridge, Tennessee. MCNPX Code (version 2.6.0) was used to simulate fast neutron transmission of the clay materials under narrow beam geometry.

GEANT4 (GEometry ANd Tracking) is another Mente-Carlo code developed at CERN in C++ (an object-oriented programming language) for simulating the passage of elementary particles through a substance. GEANT4 can simulate particles in a very broad energy from several electronvolts to many gigaelectronvolts. It takes into account during simulation all secondary particles generated in nuclear reactions of primary particles with the substance, unlike MCNP [25].

Direct calculation of effective removal cross section, $\Sigma_R(cm^{-1})$ and mean free path λ (cm) of compounds and homogeneous mixtures is also possible from $\Sigma_{R/\rho}(cm^2g^{-1})$ value for various elements that made up the compounds or mixtures using equations (2)–(4) [19,20,26,27].

3. Methodology

3.1. Preparation of the clay-materials and elemental analysis

The two common types of clays, Kaolin and Ball clay were collected from Government Reserve Forest, Ladugbo, Ile – Ife, Southwest Nigeria (7.49°N, 4.55°E), as-mined in lump form, crushed to suitable sizes and sun-dried. The samples were pulverized, sieved (with sieve of mesh sizes 2 μm), moulded and dried in accordance to American Society for Testing and Material (ASTM) standards [12]. Carbolite Muffled Furnace was used to bake the samples at different temperatures (550 °C and 1000 °C). Fig. 1 shows Ball Clay samples labelled Sample A, B and C for the unbaked and those that were baked at 550 °C and 1000 °C respectively. Likewise, Fig. 2 shows Kaolin samples labelled Sample D, E and F for the unbaked and those that were baked at 550 °C and 1000 °C respectively.

The samples were pelletized. To determine elemental concentrations of the samples, Tandem Pelletron Accelerator (1.7 MV, Model 5SDH) was used for Particle Induced X-ray Emission (PIXE). The compositions have been listed in Table 2.

3.2. Computation of mass removal cross section, effective removal cross-section and mean free path

All the parameters required for the analysis of FNSB of the samples have been evaluated with the WinNC-Toolkit. The input elemental compositions (PIXE results) of clay-samples have been used. Computation of the toolkit is based on the Eqs. (1)–(4). The computational procedure is described in the flow chart shown below (Fig. 3).

3.3. Simulation of fast neutron transport of clay-materials using MCNPX and GEANT4 codes respectively

A simulation is an imitation of the operation of a real-world process or system [27]. In recent years, dexterities of the personal computers, as well as work-stations, authorize the application of Monte Carlo method to simulate and solve highly complex physical problems that involve the transport of different types of radiation

Table 3
Calculation of the fast neutrons effective removal cross-sections for the samples.

Ele.	$\Sigma_{R/\rho}$ (cm^2g^{-1})	Sample A Density (gcm^{-3}) = 1.99 λ (cm) = 17.33		Sample B Density (gcm^{-3}) = 1.97 λ (cm) = 17.54		Sample C Density (gcm^{-3}) = 1.96 λ (cm) = 17.82		Sample D Density (gcm^{-3}) = 1.99 λ (cm) = 17.33		Sample E Density (gcm^{-3}) = 1.97 λ (cm) = 17.48		Sample F Density (gcm^{-3}) = 1.96 λ (cm) = 17.57	
		Ele. Conc By Wt	Partial Σ_R Density (cm^{-1})	Ele. Conc By Wt	Partial Σ_R Density (cm^{-1})	Ele. Conc By Wt	Partial Σ_R Density (cm^{-1})	Ele. Conc By Wt	Partial Σ_R Density (cm^{-1})	Ele. Conc By Wt	Partial Σ_R Density (cm^{-1})	Ele. Conc By Wt	Partial Σ_R Density (cm^{-1})
Mg	3.33E-02	1.44E-02	2.86E-02	1.44E-02	2.84E-02	1.11E-02	2.18E-02	7.26E-04	0.00E+00	0.00E+00	0.00E+00	0.00E+00	0.00E+00
Al	2.93E-02	3.54E-01	7.04E-01	2.38E-01	4.69E-01	2.08E-01	4.07E-01	1.19E-02	3.59E-01	7.15E-01	2.09E-02	3.51E-01	6.91E-01	2.03E-02	3.61E-01	7.07E-01	2.07E-02
Si	2.96E-02	5.59E-01	1.11E+00	6.59E-01	1.30E+00	6.39E-01	1.25E+00	3.71E-02	5.52E-01	1.10E+00	3.25E-02	5.68E-01	1.12E+00	3.31E-02	5.58E-01	1.09E+00	3.24E-02
P	2.82E-02	0.00E+00	0.00E+00	3.32E-04	6.53E-04	2.96E-02	5.79E-02	1.63E-03	0.00E+00	0.00E+00	0.00E+00	0.00E+00	0.00E+00	0.00E+00	0.00E+00	0.00E+00	0.00E+00
Cl	2.52E-02	6.40E-04	1.27E-03	4.12E-04	8.12E-04	4.69E-03	9.20E-03	2.32E-04	7.04E-04	1.40E-03	3.53E-05	0.00E+00	0.00E+00	0.00E+00	0.00E+00	0.00E+00	0.00E+00
K	2.47E-02	1.74E-02	3.47E-02	2.19E-02	4.31E-02	1.34E-02	2.62E-02	6.46E-04	6.68E-02	1.33E-01	3.28E-03	6.59E-02	1.30E-01	3.21E-03	6.53E-02	1.28E-01	3.16E-03
Ca	2.43E-02	2.70E-03	5.37E-03	1.31E-04	3.19E-03	6.29E-03	1.53E-04	2.96E-04	5.80E-04	1.41E-05	2.79E-03	5.55E-03	1.35E-04	1.28E-03	2.51E-03	6.11E-05	1.31E-03	2.56E-03	6.22E-05
Ti	2.05E-02	8.58E-03	1.71E-02	3.50E-04	1.09E-02	2.15E-02	4.41E-04	1.97E-04	3.86E-04	7.92E-06	5.12E-04	1.02E-03	2.09E-05	4.73E-04	9.32E-04	1.91E-05	5.04E-04	9.87E-04	2.02E-05
V	2.13E-02	1.56E-04	3.10E-04	6.60E-06	0.00E+00	0.00E+00	0.00E+00	8.79E-04	1.72E-03	3.67E-05	0.00E+00	0.00E+00	0.00E+00	0.00E+00	0.00E+00	0.00E+00	7.28E-05	1.43E-04	3.04E-06
Cr	2.09E-02	9.88E-05	1.97E-04	4.11E-06	1.21E-04	2.38E-04	4.97E-06	9.23E-02	1.81E-01	3.78E-03	4.76E-05	9.46E-05	1.98E-06	0.00E+00	0.00E+00	0.00E+00	0.00E+00	0.00E+00	0.00E+00
Mn	2.03E-02	4.58E-04	9.12E-04	1.85E-05	5.74E-04	1.13E-03	2.30E-05	2.77E-05	5.44E-05	1.10E-06	1.68E-04	3.33E-04	6.77E-06	1.03E-04	2.03E-04	4.12E-06	1.55E-04	3.04E-04	6.16E-06
Fe	2.14E-02	4.18E-02	8.32E-02	1.78E-03	4.98E-02	9.82E-02	2.10E-03	1.36E-04	2.67E-04	5.71E-06	1.68E-02	3.35E-02	7.16E-04	1.28E-02	2.52E-02	5.38E-04	1.32E-02	2.58E-02	5.53E-04
Cu	1.86E-02	1.51E-05	3.00E-05	5.58E-07	2.53E-05	4.98E-05	9.26E-07	0.00E+00	0.00E+00	0.00E+00	0.00E+00	0.00E+00	0.00E+00	0.00E+00	0.00E+00	0.00E+00	0.00E+00	0.00E+00	0.00E+00
Zn	1.83E-02	5.73E-05	1.14E-04	2.09E-06	7.78E-05	1.53E-04	2.80E-06	0.00E+00	0.00E+00	0.00E+00	1.26E-04	2.52E-04	4.60E-06	7.34E-05	1.45E-04	2.65E-06	9.98E-05	1.96E-04	3.58E-06
Rb	1.64E-02	1.05E-04	2.08E-04	3.41E-06	1.01E-04	1.99E-04	3.26E-06	1.11E-03	2.17E-03	3.56E-05	6.32E-04	1.26E-03	2.06E-05	4.69E-04	9.23E-04	1.51E-05	5.86E-04	1.15E-03	1.88E-05
Zr	1.56E-02	4.56E-04	9.08E-04	1.42E-05	8.61E-04	1.70E-03	2.65E-05	0.00E+00	0.00E+00	0.00E+00	0.00E+00	0.00E+00	0.00E+00	0.00E+00	0.00E+00	0.00E+00	0.00E+00	0.00E+00	0.00E+00
Total		**1.0000**	**0.0577**	**1.0000**	**0.0570**	**1.0000**	**0.0561**	**1.0000**	**0.0577**	**1.0000**	**0.0572**	**1.0000**	**0.0569**

Table 4
The WinNC-Toolkit, MCNPX, GEANT4 and calculated values of effective removal cross section, $\Sigma_R(cm^{-1})$.

Sample	WinNc $\Sigma_{R\ WinNC}\ (cm^{-1})$	MCNPX (version 2.6.0) $\Sigma_{R\ MCNPX}\ (cm^{-1})$	GEANT4 $\Sigma_{R\ Geant4}\ (cm^{-1})$	Calc. $\Sigma_{R\ Calc}(cm^{-1})$
A	0.0575	0.0581	0.0762	0.0577
B	0.0567	0.0578	0.0751	0.0570
C	0.0559	0.0567	0.0736	0.0561
D	0.0575	0.0582	0.0762	0.0577
E	0.0570	0.0576	0.0752	0.0572
F	0.0568	0.0574	0.0751	0.0569

such as gamma and neutron through matter. The codes simulate the interaction of elementary particles (such as neutrons, photons, electrons, etc) with the substance of the system. MCNPX and GEANT4 are well-known Monte Carlo codes utilized in nuclear physics, nuclear engineering and medical physics [28–38].

Fig. 4 shows the simulation set up, paraffin box as neutron source housing with a cylinder collimator. The detector was putted on the same line at a distance 70 cm from neutron source. The investigated clay materials were located between the source and the detector at a distance 50 cm from the source.

3.4. Calculation of effective removal cross-section and mean free path

From the value of mass removal cross section $\Sigma_{R/\rho}(cm^2g^{-1})$ for each elements that constituent the clay materials and the elemental compositions (PIXE results) of the samples, the effective removal cross section, $\Sigma_R(cm^{-1})$, and mean free path λ (cm) of the samples were calculated using equations (2)–(4).

4. Results and discussion

4.1. Elemental analysis

The PIXE results for ball clay (Sample A, B and C) and kaolin (Sample D, E and F) have been listed in Table 2. The results show that the clay-materials are majorly made up of silica, alumina and appreciable concentration of iron, alkali and alkaline earth minerals. The results show that the concentration of Aluminum in Kaolin is approximately twice than that in Ball clay, while there is about 9% of iron in Ball clay but iron concentration is almost insignificant in Kaolin. However, there is average 7% of Calcium in Kaolin and it is missing in Ball clay. The measured elemental-compositions of samples show good agreement with literature values [13,39]. It has been found that the effect of temperature is negligible on the sample's chemical compositions. This is again in good agreement with literature [12,13]. This supports the good refractoriness property of a clay material [40]. That is, a refractory material is one which has the ability to maintain its mechanical and chemical integrity at different temperatures.

4.2. WinNC-toolkit output

Firstly, the correctness of the WinNC-Toolkit code has been validated. This validation has been made by comparing the computed, manually calculated and experimentally measured values of effective removal cross-sections for different concrete samples [15]. These values are listed in Table 1. The mass removal cross section, effective removal cross-section and mean free path λ for Ball clay (Sample A, B, and C) and Kaolin (Sample D, E and F) have been obtained and listed in Table 2. These parameters are more or less the same for the two clay-materials baked at different temperatures. Thus supports the refractory nature of clay material as pointed out by elemental concentration results. The effective removal cross-section and mean free path for each of the samples obtained have been compared with standard concrete materials [7] as shown in Figs. 5 and 6 respectively.

4.3. Calculated effective removal cross section, $\Sigma_R(cm^{-1})$ and mean free path λ (cm)

The elemental composition, its fraction weight, mass removal cross-section $\Sigma_{R/\rho}(cm^2g^{-1})$, partial density ρ_i , macroscopic effective removal cross-section, $\Sigma_R(cm^{-1})$, and mean free path λ (cm) of fast neutrons for the samples are listed in Table 3. It is obvious that the macroscopic effective removal cross-section, $\Sigma_R(cm^{-1})$, and the mean free path λ (cm) for all the samples are apparently the same. The contribution of the light elements to the parameters is more important compare with the heavy elements.

4.4. The WinNC-Toolkit, MCNPX, GEANT4 and calculated effective removal cross section, $\Sigma_R(cm^{-1})$ compared

The comparison of the calculated macroscopic effective removal cross section values, the WinNc-Toolkit results, as well as the MCNPX and GEANT4 simulation results are shown on Table 4. The results have similar trend. The little discrepancies between MCNPX and GEANT4 values is not new, some research works have affirmed possibility of this happening [41,42].

5. Conclusions

It has been concluded from the relative comparisons of $\Sigma_R(cm^{-1})$ and λ values for the samples and standard concrete materials that the clay-materials have relatively fair FNSB. Thus taking cognizance of some factors such as availability, cost, thermo-chemical stability and good physiochemical properties of clay-materials, clay can be used for cost-effective neutron-shielding purpose at nuclear facilities.

Appendix A. Supplementary data

Supplementary data to this article can be found online at https://doi.org/10.1016/j.net.2019.03.019.

References

[1] IAEA, Harmony — the future of electricity, IAEA Bull. 25 (November 2017) 24–25.
[2] E.J. Hall, Radiobiology for the Radiologist, fifth ed., Lippincott williams & wilkins, Philadephia, 2000. New Yoke.
[3] J.E. Turner, Atoms, Radiation and Radiation Protection, third ed., John wiley and sons, New York, 2007.
[4] G.F. Knoll, Radiation Detection and Measurement, third ed., John wiley and sons, New York, 2000.
[5] R.D. Evans, in: THM (Ed.), The Atom Nucleus, McGraw-Hill, New York, 1995.
[6] E.P. Miller, Radiation Attenuation Characteristics of Structural Concrete, OAK RIDGE NATIONAL LABORATORY, Tennessee, 1958.
[7] E. Yilmaz, et al., Gamma ray and neutron-shielding properties of some

concrete materials, Ann. Nucl. Energy 38 (2011) 2204–2212.
[8] A.M. El-Khayatt, NXcom – a program for calculating attenuation coefficients of fast-neutrons, Ann. Nucl. Energy 38 (2011) 128–132.
[9] N.A. Alallak, Factors affecting gamma ray transmission, Jordan J. Phys. 5 (2012) 77–88.
[10] K.S. Mann, Gamma-ray shielding behaviours of some nuclear engineering materials, Nucl. Eng. Tech. 49 (2017) 792–800.
[11] Oak ridge national laboratory, Early Test Facilities and Analytic Methods. *Special Session Radiation Protection and Shielding*, US, Department of energy, Chicago, 1992, pp. 1–8.
[12] S.A. Agbalajobi, Analysis on some physical and chemical properties of Oreke dolomite deposit, J. Miner. Mater. Charact. Eng. 1 (2013) 33–38.
[13] J.A. Omotoyinbo, Working properties of some selected refractory clay deposits in southwestern Nigeria, J. Miner. Mater. Charact. Eng. 7 (2008) 233–245.
[14] O.S. Adegoke, Guide to the Non-metal Mineral Industrial Potential of Nigeria. Raw Materials Research and Development Council, RMRDC, Kaduna, Nigeria, 1980, pp. 110–120.
[15] K.S. Mann, Fast-neutron removal cross-section calculations: computer program, Int. J. Appl. Innovat. Eng. Manag. 6 (2015).
[16] MCNP X-5, A General Monte Carlo N-Particle Transport Code: V. 5, vol. I (LA-UR-03e1987) and vol. II (LACP-0245), Los Alamos National Laboratory, 2003.
[17] A.N. Solovyev, et al., Comparative analysis of MCNPX and GEANT4 codes for fast-neutron radiation treatment planning, Nucl. Energy Technol. 1 (2015) 14–19.
[18] M.F. Kaplan, Concrete Radiation Shielding, Wiley, New York, 1989.
[19] Y. Elmahroug, Calculation of fast-neutron removal cross-sections for different shielding materials, Int. J. Phys. Res. 3 (2013) 7–16.
[20] Y. Elmahroug, Calculation of gamma and neutron-shielding parameters for some materials polyethyleneased, Int. J. Phys. Res. 3 (2013) 33–40.
[21] S.M. Harjinder, Experimental investigation of clay fly-ash bricks for gamma-ray shielding, Nucl. Energy Technol. 48 (2016) 1230–1236.
[22] M.J. Berger, J.H. Hubbell, WinXCom Software, Version 1.0.1, 1999.
[24] S.G. Sesonske, Nuclear Reactor Engineering, fourth ed., Chapman & Hall Inc, London, 1994.
[25] Geant4: a toolkit for the simulation of the passage of particles through matter, Available at: http://geant4.cern.ch/.
[26] A.E. Profio, Radiation Shielding and Dosimetry, Wiley, New York, 1982.
[27] J. Banks, Discrete-Event System Simulation, Prentice Hall, 2001, ISBN 0-13-088702-1, p. 3.
[28] H.O. Tekin, V.P. Singh, T. Manici, Effects of micro-sized and nano-sized WO_3 on mass attenuation coefficients of concrete by using MCNPX code, Appl. Radiat. Isot. 121 (2017) 122–125. https://doi.org/10.1016/j.apradiso.2016.12.040.
[29] H.O. Tekin, T. Manici, Simulations of mass attenuation coefficients for shielding materials using the MCNP-X code, Nuclear Science and Techniques. NUCL SCI TECH 28 (2017) 95, https://doi.org/10.1007/s41365-017-0253-4.
[30] G. Lakshminarayana, S.O. Baki, Kawa M. Kaky, M.I. Sayyed, H.O. Tekin, A. Lira, I.V. Kityk, M.A. Mahdi, Investigation of structural, thermal properties and shielding parameters for multi-component borate glasses for gamma and neutron radiation shielding applications, J. Non-Cryst. Solids (2017). https://doi.org/10.1016/j.jnoncrysol.2017.06.001.
[31] M.G. Dong, E. El-Mallawany, M.I. Sayyed, H.O. Tekin, Shielding properties of 80TeO2–5TiO2–(15–x) WO3–xAnOmglassesusingWinXComand MCNP5 code, Radiat. Phys. Chem. 141 (2017) 172–178. https://doi.org/10.1016/j.radphyschem.2017.07.006.
[32] H.O. Tekin, M.I. Sayyed, Shams A.M. Issa, Gamma radiation shielding properties of the hematite-serpentine concrete blended with WO_3 and Bi_2O_3 micro and nanoparticles using MCNPX code, RadiationPhysicsandChemistry 150 (2018) 95–100. https://doi.org/10.1016/j.radphyschem.2018.05.002.
[33] M.I. Sayyed, H.O. Tekin, O. Kilicoglu, O. Agar, M.H.M. Zaid, Shielding features of concrete types containing sepiolite mineral: comprehensive study on experimental, XCOM and MCNPX results, Results in Physics 11 (2018) 40–45. https://doi.org/10.1016/j.rinp.2018.08.029.
[34] M.I. Sayyed, Y.S. Rammah, A.S. Abouhaswa, H.O. Tekin, B.O. Elbashir, ZnO-B2O3-PbO glasses: synthesis and radiation shielding characterization, Physica B: *Phys. Condens. Matter* (15 August 2018). Available Online, https://doi.org/10.1016/j.physb.2018.08.024.
[35] J. Allison, et al., Geant4 developments and applications, IEEE Trans. Nucl. Sci. 53 (1) (2006) 270–278.
[36] K. Amako, et al., Comparison of Geant4 electromagnetic physics models against NIST reference data, IEEE Trans. Nucl. Sci. 52 (4) (2005) 218–910.
[37] S. Jan, et al., GATE: a simulation toolkit for PET and SPECT, Phys. Med. Biol. 49 (2004) 4543–4561.
[38] G. Santin, V. Ivanchenko, et al., GRAS: a general-purpose 3-D modular simulation tool for space environment effect analysis, IEEE Trans. Nucl. Sci. 52 (6) (2005) 2294–2299.
[39] E. Nnuka, C. Enejor, Characterisation of Nahuta clay for industrial and commercial applications, Niger. J. Eng. Mater. 2 (2001) 9–12.
[40] J.H. Chester, Refractories, Production and Properties, The Iron and Steel Institute, London, 1973, pp. 4–13, 295 – 315.
[41] I.I. Bashter, Calculation of radiation attenuation coefficients for shielding concretes, Ann. Nucl. Energy 24 (1997) 1389–1401.
[42] B.M. van der Ende, et al., Use of GEANT4 vs. MCNPX for the characterization of a boron-lined neutron detector, Nucl. Instrum. Methods Phys. Res. 820 (2016) 40–47.